

Human-robot collaborative site-specific sprayer

Ron Berenstein  | Yael Edan

Ben-Gurion University of the Negev,
Beer-Sheva, 8410501, Israel

Correspondence

Ron Berenstein, Department of Industrial
Engineering and Management, Ben-Gurion
University of the Negev, Beer-Sheva 8410501,
Israel.

Email: berensti@bgu.ac.il

Abstract

Spraying pesticides is a key element of agriculture worldwide, since 30% to 35% of crop losses can be prevented when harmful insects and diseases are eliminated by applying pesticides. Site-specific spraying can help reduce pesticide application; however, target detection is limited due to the complex agricultural environment. This paper presents a human-robot collaborative sprayer designed for site-specific targeted spraying. The robotic sprayer platform, the framework, and tools for the robotic sprayer to collaborate with a remote human operator for the target detection and spraying tasks are detailed. An experiment to evaluate the elements of the collaborative human-robot framework working in sync was designed, implemented, and evaluated. The collaborative spraying system shows a 50% reduction of sprayed material. The experiment also proves the feasibility of human-robot collaboration for the complex task of spraying specific targets considering both the True Positive (TP) and False Positive (FP) rates.

KEYWORDS

agriculture, human robot interaction, machine vision, Spraying, wheeled robots

1 | INTRODUCTION

Application of nutrients, fungicides, and pesticides is one of the most important processes in agricultural production, and it can have a significant impact on crop yield, quality, and ultimately profitability.¹ It is estimated that approximately 30%–35% of crop losses can be prevented when harmful insects and diseases are eliminated by applying pesticides.²

Current methods for pesticide application include a human operator traveling along the crop rows and selectively spraying the targets manually using a backpack sprayer (Fig. 1, left), but a more commonly used method is mechanized nonselective spraying in which a human drives a tractor with a sprayer connected to the tractor that sprays the crops continuously (Fig. 1, right). Despite the use of pesticide protection equipment (a personal head mask and a central filtration system for the manual and mechanized spraying methods, respectively), the human is still exposed to hazardous pesticides that can cause negative health issues.³

Robotic technology can provide a way to reduce the quantity of pesticide applied, improve its sustainability, and reduce its environmental impact.⁴ A target-specific robotic sprayer can reduce the quantity of pesticides applied in modern agriculture and potentially remove or minimize the human presence during the pesticide spraying process.⁵ Studies show that up to 60% of pesticide use can be reduced when the spraying material is targeted toward the designated object.^{6–8}

Agricultural robots have been developed for many operations, such as field cultivation, planting, spraying, pruning, and selective



FIGURE 1 Pesticide spraying methods. Backpack sprayer (left) where the human carries the pesticide and sprays each target manually, and tractor sprayer (right) where the human drives a tractor with spraying equipment

harvesting.^{9–11} A comprehensive review of the state-of-the-art harvesting robots for high-value crops¹² identifies three sources of variation in a crop environment that must be considered in the development of a harvesting robot: objects, environment, and crops.

Robotic systems for spraying in agriculture have been developed for plant protection applications, for weeding, and other similar tasks. A robotic weed control system that mechanically cuts a targeted weed while applying a minute amount of chemical to the cut surface of the weed has been developed.¹³ Although the robotic system showed great potential in site-specific weed management, there is still a gap in the development of a commercial robot. A review on autonomous robotic weed control systems⁴ describes the current status of the four core technologies (guidance, detection and identification, precision in-row weed control, and mapping) required for the successful

development of a general-purpose robotic system for weed control. The authors conclude that while a few complete robotic weed control systems have demonstrated the potential of the technology in the field, additional research and development is needed to fully realize this potential. A scaled-down prototype consisting of a visually controlled robotic arm that guides the jet of a mounted sprayer directly toward date clusters completely autonomously and from a short distance¹⁴ presents a great way to extract the human operator from hazardous environments such as pesticides.

The two core tasks for agricultural spraying robots are sensing—for target detection, and “robotics”—for the spray execution.¹⁵ In this work, a fully operational robotic sprayer integrating both tasks into an operational system is demonstrated. To ensure a simple system design, a single RGB camera was used for the sensing, and a fully operational robotic platform was used for the robotic part.

Extensive work has been conducted on object detection in complex agricultural environments,¹⁶ but detection rates in real-world conditions remain limited to a 90% true positive (TP) rate and are often much lower.^{12,16–18} The limited performance is caused by the complicated agricultural conditions^{15,16,18} due to the high variability of the agricultural objects (i.e., color, texture, orientation), their amorphous size and shape, and the unstructured and dynamic environmental conditions (e.g., changing illumination directions, shading, and targets occlusion). Recent work¹⁹ showed a 95% TP rate for detecting red grape clusters, but with an artificial white screen as a background (to avoid confounding effects from the background vegetation); it is reasonable to assume that the TP rate performance of these algorithms will be different under real-world conditions and for green grapes. According to previous work,²⁰ in order for the robot to be economically feasible it must be able to detect and spray more than 95% of the targets successfully.

Unlike robotic sprayers, humans can easily adapt to such changing environments due to their high perception skills. By taking advantage of human perception skills and incorporating them with the robot's accuracy and consistency, a combined human-robotic system can be simplified and result in improved performance.^{21,22} Human-robot collaboration has been proven to improve detection and reduce cycle time.²³ A teleoperated system for navigating a crawler robotic vehicle along predefined paths with two modes of control—direct and supervisory—was developed.²⁴ Results indicated that direct control was difficult for the operator due to the high delay time between the operator command and the robotic response. The supervisory mode showed the ability to travel straight with a maximum lateral error of 0.3 m. Recent work²⁵ performed in parallel to this research focused on human-robot interaction aspects as applied to a teleoperated system. The research provided design principles for developing a teleoperated user interface for an agricultural sprayer^{26,27} based on a focused literature review, and it involved the collection of robot teleoperation interface design guidelines, user-centered methods, and field experience.

To improve robotic targeted spraying, a human-robot collaborative sprayer has been developed.²⁸ It includes several levels of collaboration based on Sheridan's 10 levels of collaboration.²⁹ The human-robot collaborative sprayer presented in this paper integrates all modules necessary for site-specific spraying: target detection

algorithms, target marking techniques,³⁰ a remote interface for human-robot collaboration,³¹ collaboration levels between the human and the robot,³² and an adjustable diameter spraying device.³³ The proposed human-robot collaborative framework focuses on the main task of **detecting and spraying targets**, with the aim to **increase TP rate** and **reduce false positives (FPs)**.

Most agricultural robotics research to date focused only on TP rates.¹² It is known that there is a tradeoff between TP and FP rates.³⁴ Furthermore, an increased number of FPs leads to increased cycle times and wasted spray material. Hence, it is important to ensure a decrease of FP rates while increasing the TP rate.

The motivation for the proposed system was to remove the human from the hazardous pesticide environment and to reduce the use of pesticides by minimizing the quantity of sprayed material (minimizing FPs) while maintaining the crop yield (maximizing TP rate). A robotic sprayer platform was designed and built to serve as a research tool for investigating methods and devices designated for the agricultural domain in general and specifically for vineyards operations. A human-robot framework for the target detection task was designed, implemented, and evaluated. This included a user interface and communication infrastructure developed to enable a remote operator to communicate and collaborate with the remote robot. The field experiments conducted and presented in this paper provide insights on the full operation of a human-robot collaborative system operating in the agricultural domain.

2 | HUMAN-ROBOT FRAMEWORK

2.1 | Overview

The human and the robot work collaboratively to detect artificial targets (Fig. 9) in a sequential mode as described in the workflow diagram presented in Figure 2. A target detection algorithm is operated on images acquired in the field by the robotic platform. The framework poses the human at a remote location equipped with a target-marking device (e.g., a stationary computer, laptop, tablet, PDA, or smart phone), and it uses the human's excellent perception skills to mark targets on images captured by the robot in the field. Depending on the collaboration level (described below), the human can mark additional targets and/or erase targets detected by the imaging algorithm. The marked targets are then sent back to the robot for actual spraying. Two different marking methods are proposed, implemented, and evaluated.

2.2 | Human target-marking

Two marking methods were implemented based on results from previous work:³⁰ Marking method I—*Constant Diameter Circle (CDC)*: the operator sets the center of a preset constant diameter circle, and by clicking the left button on the mouse, the circle is marked on the image (Fig. 3, upper left). Using this method, the operator cannot change the circle diameter. Marking method II—*Free-hand marking*: the operator clicks the left button on the mouse (without release) and surrounds

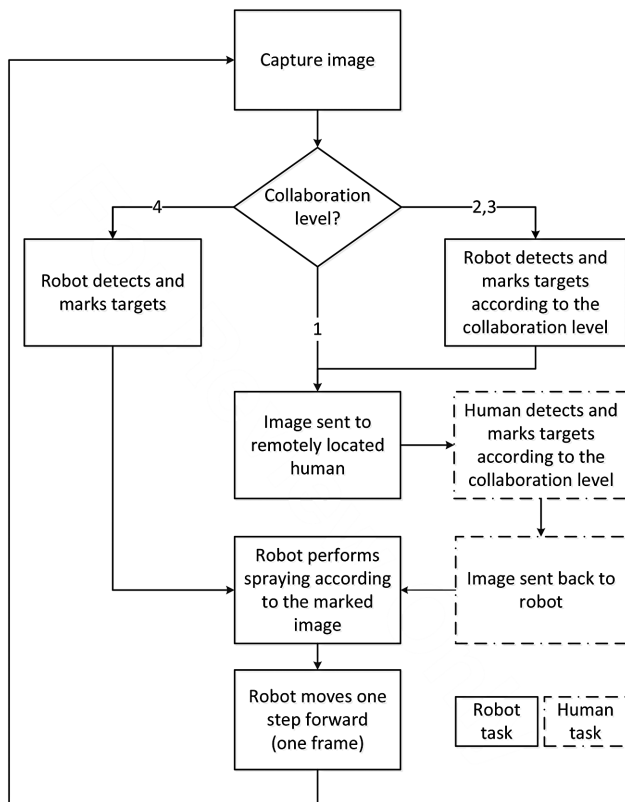


FIGURE 2 Human-robot collaboration workflow diagram. The flow diagram presents the task allocation between the robot in the field and the remote human operator (collaboration levels 2, 3, and 4 are described in Section 2.3)

the target area. When releasing the mouse button, the area bounded is marked as a target (Fig. 3, upper right). In each method, the area bounded within the marked area is considered as “detected” and colored in red. While using each of the marking methods, the operator can use the right button on the mouse to erase a marked target. The erasing method is identical to the marking method (e.g., when using the CDC method, the operator can click the right button on the mouse and the target marked within that area will be erased).

When the target marking process is completed (due to marking all the targets or at the end of the marking time for the image), a binary image is produced for the robot indicating the targets to be sprayed (Fig. 3, lower left and right).

2.3 | Human-robot collaboration

The human-robot collaborative target detection task was defined so as to ensure a high TP rate and a low FP rate. The human’s task was to assist the robot with the target detection, and the robot’s task was to detect targets and perform the actual spraying procedure. Four levels of human-robot collaboration were developed based on Sheridan’s 10 levels of human-robot collaboration²⁹ and on previous simulation analyses,³⁵ which evaluated the adaptation of these levels for target recognition. The levels are sorted by increasing robot autonomy alongside decreasing human supervision.

Collaboration level 1: fully manual human target marking. A raw image from the field is sent directly to the remotely located human operator. The operator’s task is to mark the targets in the image within the time limitation. All targets marked by the operator are sprayed.

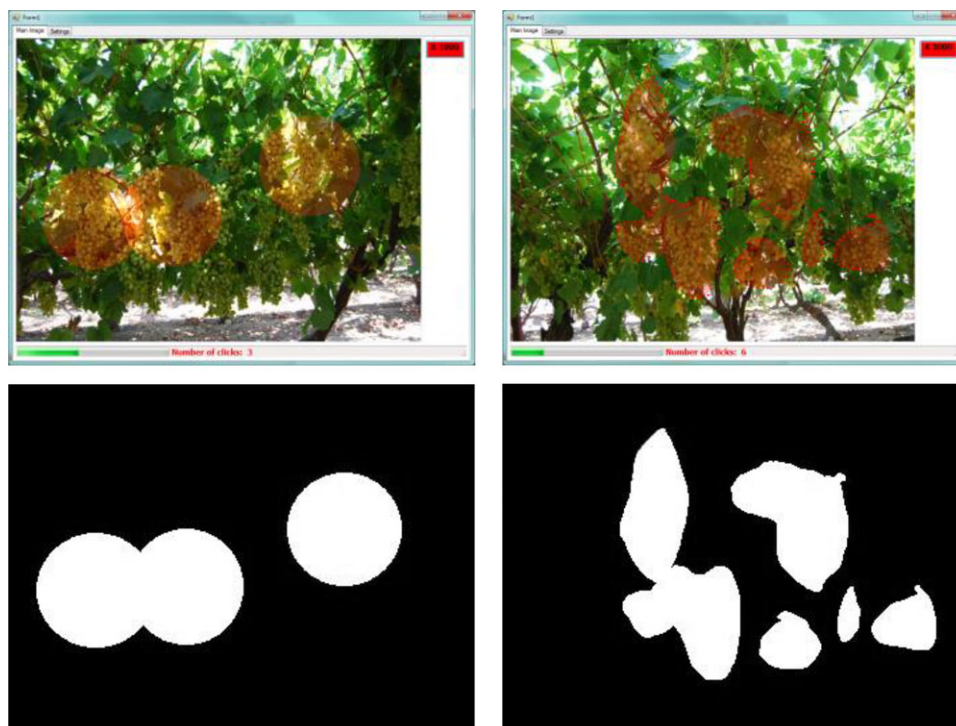


FIGURE 3 Marking methods. CDC (upper left), free-hand (upper right), CDC result (lower left), and free-hand result (lower right). The targets to be marked are the grape clusters

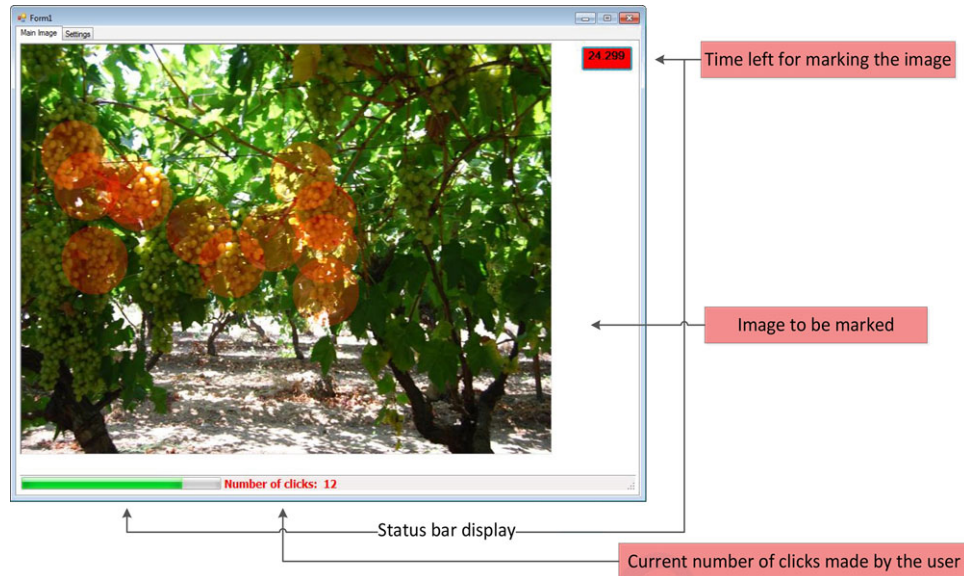


FIGURE 4 User interface for the remote human operator

Collaboration level 2: robot suggests, human approves. The image captured in the field is processed by the robotic target detection algorithm. Detected objects are considered as recommendations for the human operator and are colored in a partially transparent blue hue. After the robot detection process, the marked image is sent to the operator. The human operator must mark each target he/she wants to spray. The operator can use the robot-recommended areas in order to achieve an enhanced target TP rate. All areas to be sprayed must be marked by the human.

Collaboration level 3: robot marks, human supervises. The captured image from the field is processed by the robotic target detection algorithm. These marked areas are considered target areas that should be sprayed and are colored with a partially transparent red hue, exactly like the human marking color. After the robot detection process, the marked image is sent to the human. The human operator can add, change, and erase the robot's markings. If the human does not make any change in the robot-marked image, all the robot-marked areas will be considered targets and will be sprayed.

Collaboration level 4: fully autonomous robot marking. This collaboration level is the highest according to Sheridan,²⁹ in which the human does not have a part in the target detection process. The robot detects the target and accordingly the sprayer is directed toward each object.

2.4 | User interface design

The main goal of the interface is to present the human with images captured by the robot in the field. Using one of the suggested marking methods, the human marks targets within the image; the images are presented to the user within a constant time frame that corresponds to the advancing speed of the sprayer along the field.

The interface (Fig. 4), consisting of a single window in which the user can mark the targets according to the preselected marking method, was designed using Microsoft Visual Studio IDE (C#) under the Windows 7 operating system. The interface includes two indicators for the

user. The first indicator is the time left for marking the current image in the form of a slide bar located at the bottom of the interface. The second indicator is a button located at the upper right corner of the interface, which is used to establish a remote connection with the robot. The default background color of the button is gray. When the button is pressed, the background color changes to orange, indicating that the server is running and waiting for communication from the robot (the robot is considered a client). Once the robot is ready for the spraying process, it initiates communication with the interface. When communication between the remote interface and the robot in the field is established, the button background color changes to red.

3 | THE ROBOT

A robotic platform was designed and built to serve as a research tool for investigating methods and devices designated for the agricultural domain in general and specifically for vineyard operations.²⁸ Detecting and spraying the grape clusters was the main agricultural task. The robot was designed to include all the necessary equipment, hardware, and software required to accomplish autonomous and semiautonomous (human-assisted) field tasks such as navigation along the vineyard row and spraying accurately toward the target area.

The robotic chassis (Fig. 5, left) is assembled from two identical platforms that are interconnected using a two-degree-of-freedom (2DOF) universal joint (Cardan joint). The first DOF is used to improve the turning radius, and the second allows the platform designers to neglect the need for a complicated suspension system. Although the robot is capable of turning using differential steering, allowing a relative angle between the platforms contributes to a smaller turning radius and minimizes side slip of the wheels, resulting in reduced wear of the vehicle and less ground trace. The platform payload is designed for 300 kg. A modular approach is taken with four identical wheel modules. Each wheel module consists of the following: an ATV wheel (0.5 m

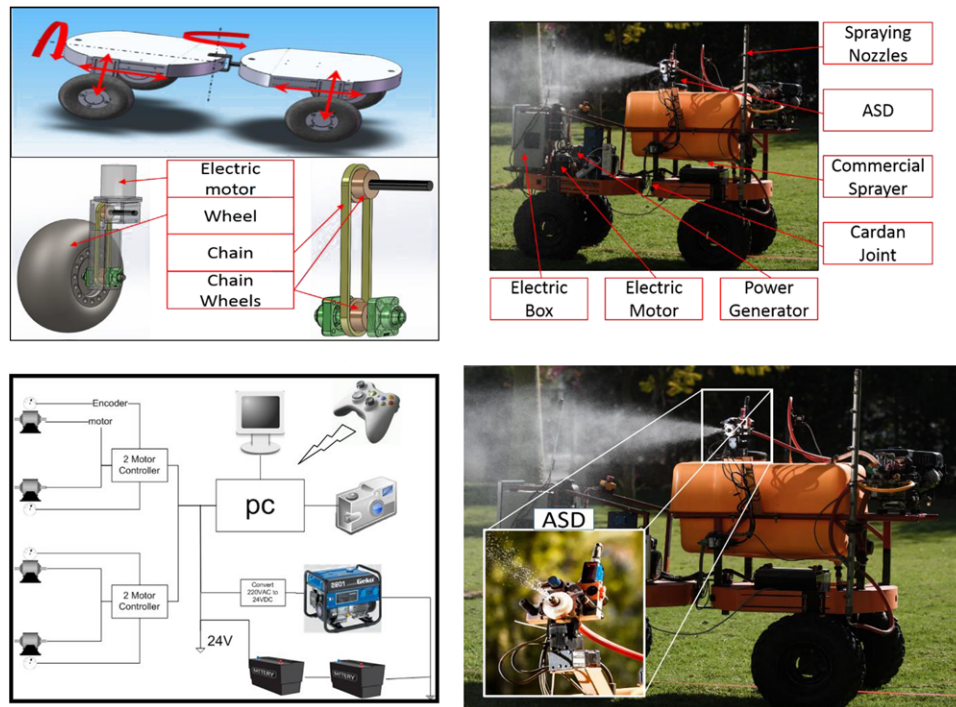


FIGURE 5 Robotic sprayer. CAD drawing of two identical platforms interconnected using a 2DOF universal joint and wheel unit (upper left), complete robotic sprayer with all of the main components and peripheral accessories attached (upper right), robotic sprayer electric power scheme (lower left), and a focused ASD image within the overall robotic sprayer (lower right)

diameter), a wheel shoulder that connects the wheel to the platform, and a 24 V–480 W electric motor. The electric motor is fixed to the platform and connected to the wheel using chain wheels. Using incremental encoders connected to each wheel, the wheel position and speed can be controlled using a developed kinematic model.^{28,36}

The robot is equipped with an electrical box that is mounted to the front platform and contains the following: a PC with an i7 processor, a 7-in. touch screen, two electric motor controllers (Roboteq AX3500), and some small peripheral aids (e.g., Arduino boards and a step motor controller). Other equipment is mounted to the platform, including two color cameras (Microsoft LifeCam Studio) (one facing forward for navigation and the second facing sideways for target detection), two 12 V 110A/h car batteries, a 2500W (Geko 2801) power generator, and a commercial sprayer (a 200 L tank with an internal combustion engine connected to a liquid pressure pump). A gamepad controller (Microsoft Xbox 360) is connected wirelessly to the robot platform and used for manual maneuvering of the robotic platform.

The robot uses a fanless spraying design in order to minimize the spraying drift and to achieve highly accurate spraying. It must be noted that agronomy experiments are necessary to validate the sprayer efficiency.

An adjustable spraying device (ASD; Fig. 5, lower right, and Fig. 6) was developed using a single nozzle (AYHSS 16) to enable accurate spraying of the agricultural target.³³ The developed device was designed to implement the one target–one shot (OTOS) spraying method, which was designed to cover the entire target by adjusting the spray diameter to the minimum possible closing circle diameter with a single spray.³⁷ The core of the ASD contains three elements: a spraying nozzle, a step motor interconnected to the nozzle, and a

camera. Based on the size of the targets detected on the image captured from the camera, the step motor changes the nozzle diameter and performs a single spray using an electric valve.³³ The ASD was mounted to a pan-tilt unit (PTU) that directs the nozzle toward the target.

The operational concept of the ASD presented in Figures 6 and 7 is described in detail in Ref. 33. An image is captured using the ASD mounted camera (Microsoft Studio with 600 × 800 resolution). Using machine vision algorithms (such as the one in Ref. 38), the center-of-mass location and the closing circle diameter of each target are calculated. Using the PTU, the ASD nozzle is directed toward the target center of mass; using a stepper motor, the nozzle aperture and the spraying diameter are adjusted. An electric valve controls the opening and closing of the spray.

4 | INTEGRATIVE SITE-SPECIFIC SPRAYER EXPERIMENT

4.1 | Overview

An experiment was designed to evaluate the human-robot collaboration framework for the site-specific target spraying task, focusing on the integrative performance of the three main components of the collaboration framework that were previously tested and evaluated separately: human marking methods,³⁰ levels of human-robot collaboration,³² and the spraying device.³³ For simplification and better control and evaluation, artificial targets were set in an artificial outdoor environment. The human-robot task was to spray the targets as

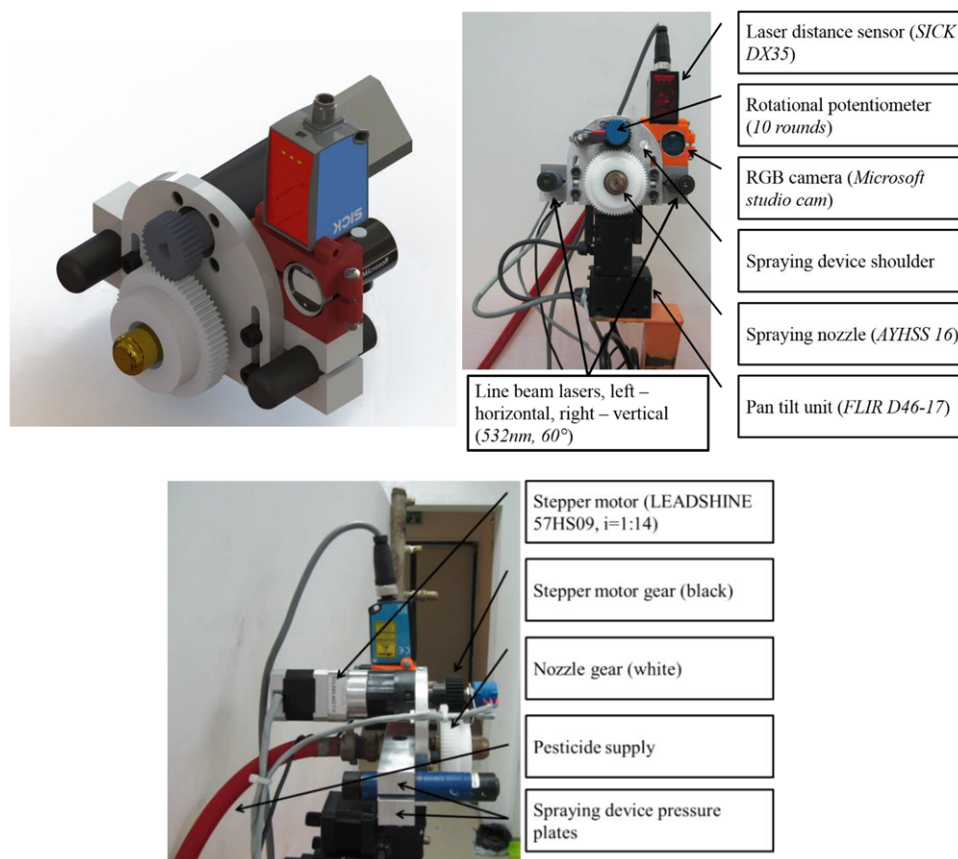


FIGURE 6 Adjustable spraying device. CAD view of the ASD (upper left), front view of the ASD mounted to a PTU (upper right), and side view of the ASD (lower middle)

accurately as possible, within a limited time frame that corresponded to the sprayer speed as it advanced along the row. To simulate real-world conditions, the human operator was located at Ben-Gurion University of the Negev, Beer-Sheva, Israel, 90 km south of the robotic platform, which was located at Beit-Dagan, Israel.

4.2 | Robot side

To focus on the target detection/spraying tasks, the robotic platform was programmed to autonomously follow a red base line (a red plastic strip of 50 mm width) that was fixed at a 1.6 m distance in parallel to the target's base (Fig. 8, left). During each step, the robot travels 1 m to completely change the current frame point of view (POV). The robot's travel speed was set to 0.2 m/s. The ASD was mounted to the robot, perpendicular to the robot's travel direction, facing the target's base (Fig. 8). Fifty targets were randomly spread along an 18-m-long path and were set at least 20 cm apart, imitating grape clusters.

Although the robotic sprayer was designed for spraying grape clusters,³⁸ in this experiment artificial custom targets specifically designed for the experiment were used. The use of artificial targets enabled precise detection of the targets and high target detection repetitiveness, which was essential for comparing the different experiment repetitions, users, marking methods, and collaboration levels. Another advantage of using artificial targets is that the TP and FP rates could be controlled, unlike the unstructured grape cluster scene.

The targets were constructed from blue polyethylene plastic and were hand-cut according to four shape patterns as shown in Figure 9. To be as close as possible to commercial field conditions, the experiment included predefined TP and FP rates. Two types of targets were used: 38 targets that can be detected by the robotic sprayer (targets with a red circle in the middle of the target; Fig. 10, left), and 12 targets that cannot be detected by the robotic sprayer (targets with a yellow circle in the middle of the target; Fig. 10, right).

An artificial target detection algorithm was developed specifically for detecting the artificial targets and the color of the circle in the middle (red for robot-detectable and yellow for targets not detected). The target detection algorithm was based on simple color thresholding and was implemented using Matlab software equipped with an image processing toolbox. The algorithm is based on isolating the blue target in the image (the background of the image is the target base, which is white in color) and identifying the color of the circle midtarget.

Since artificial targets are being used in this experiment, the artificial target detection algorithm can reach a 100% TP rate and close to zero FP. To match vineyard field conditions, a FP area was added to the detected target surroundings. The predefined FPs were added using the Matlab image processing tool. The mathematical morphology operation *Dilation* was used to expand the computer-detected target (Fig. 11). Since each of the captured images is unique in the sense of different numbers of targets, target orientation, and position, the added FP area is different for each image. The FP rate was set between 10%

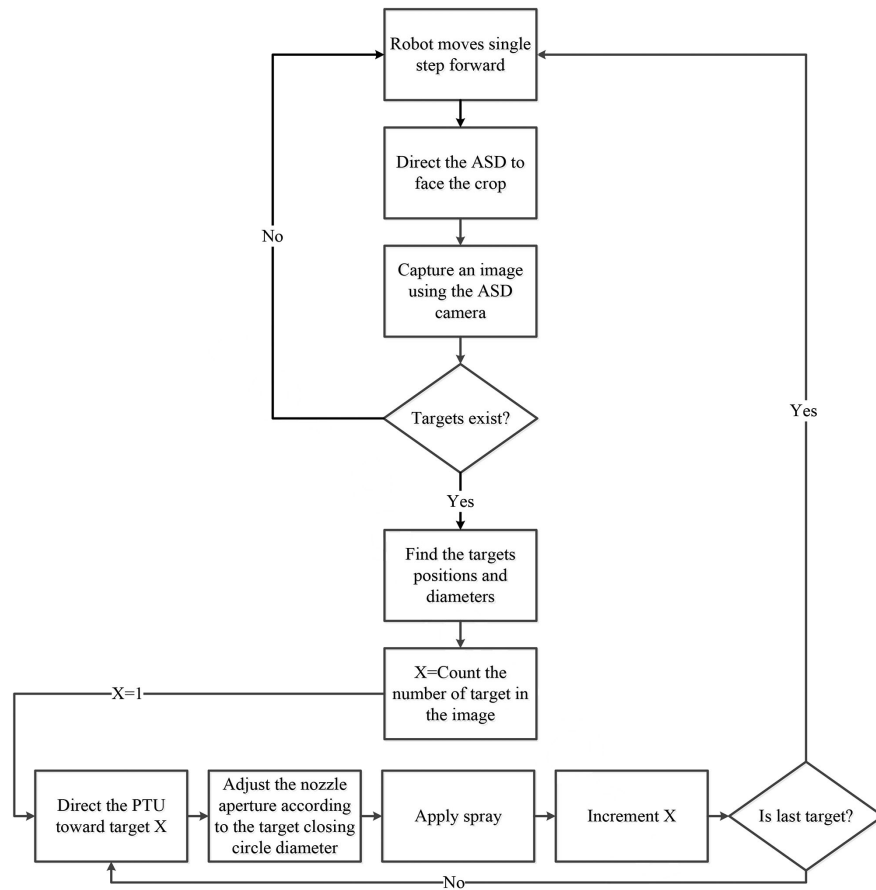


FIGURE 7 Flowchart of the ASD working procedure

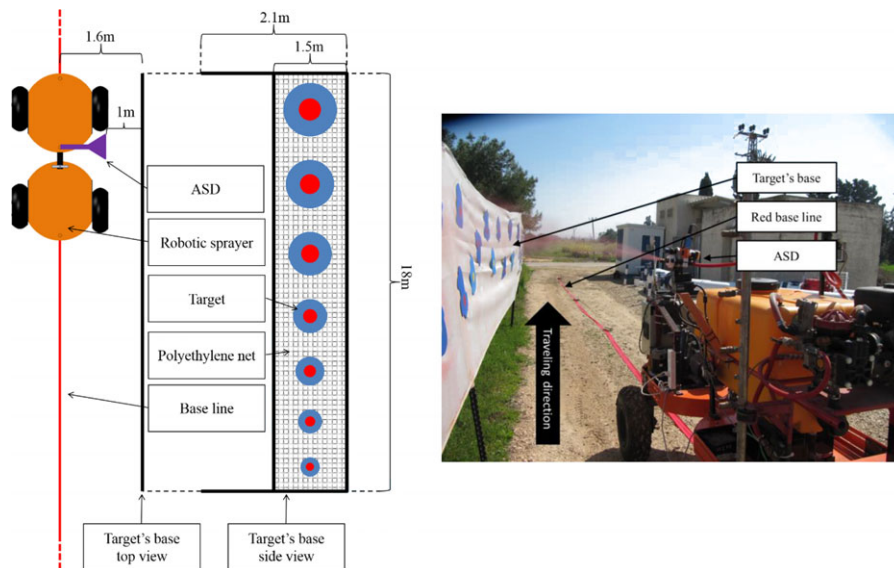


FIGURE 8 Robotic platform following red stripe. Experimental scheme including the robotic platform and target base (left) and photograph of the robotic platform during experiment (right)

and 20% according to the FP results evaluated in Ref. 38 in field conditions with an average FP of 17.3% (with a standard deviation of 5.5).

Using the ASD, the targets were sprayed with red water-soluble food dye (Florma red 696). Each target was sprayed for 1 s, and immediately after the spraying operation stopped, an image of the spray was captured and saved.

The communication between the robot and the remote human was based on the TCP-IP protocol. The robot obtained internet access using a smart phone Hot Spot (4G LTE with random switching to 3G). The remote human computer was connected to a high-speed academic network (Ben-Gurion University of the Negev Internet) with a maximum rate of 1 Gbit/s.

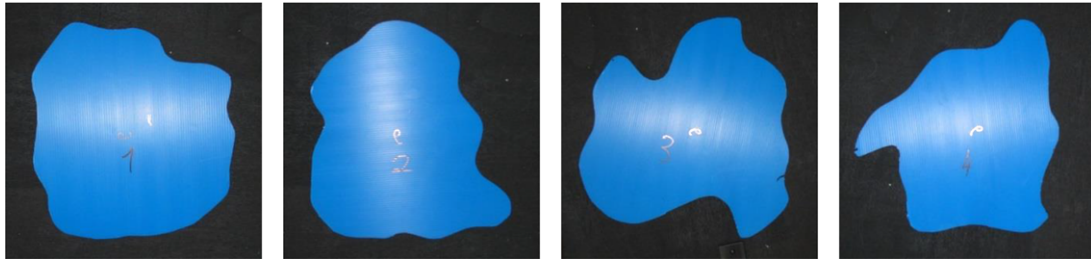


FIGURE 9 Four artificial target templates. The targets were hand-cut to obtain amorphous shapes

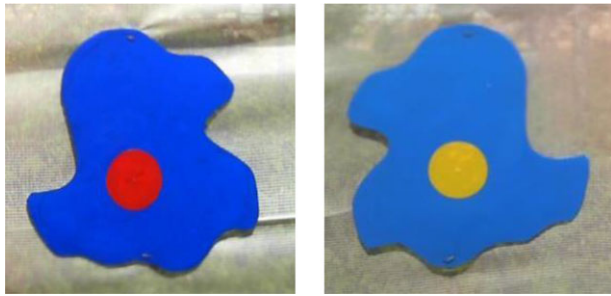


FIGURE 10 Target groups, detectable by the robot target (red circle in the center) (left) and undetectable by the robot target (yellow circle in the center) (right)

4.3 | Human task

The human task was to mark the target area using one of the marking methods and one of the suggested human-robot collaborations described above. The human used a desk computer equipped with a 21-in. screen (Fig. 12). Each user was trained before the experiment with 20 images according to the training rate evaluated in Ref. 30.

4.4 | Spray evaluation

The spraying quality was evaluated using four methods:

1. *Marking comparison*: comparison between the targets that exist in the image (Fig. 14, upper left, upper right, and lower left colored in red) and the marked areas (human and robot) (Fig. 14, lower left colored in green). The performance measures were TP and FP rates.
2. *Spraying comparison*: comparison between the targets that exist in the image (Fig. 14, upper left, upper right, and lower right colored in red) and the theoretically sprayed areas (Fig. 14, lower right colored in green). The performance measures were TP and FP rates.

3. *Qualitative evaluation*: analysis of the sprayed target (Fig. 13). Each sprayed target image was presented to an expert and was graded on a 1–5 scale (Fig. 13). The performance measure was TP rate.
4. *Spraying material estimation*: an estimation of the quantity of spraying material used (representing pesticides) was conducted based on the ASD development results.³³ In the estimation, the quantity of liquid that was used in each of the spraying experiments above is compared to a simulated experiment of the robot continuously driving along the targets' base with three open nozzles (similar to the traditional spraying method; Fig. 1, right). By multiplying the number of sprays (e.g., Table 2) with the duration of each spray (1 s) and the ASD flow-rate (0.05329 l/s), the quantity of liquid was calculated for each of the four collaboration methods. The liquid estimation of continuous spraying was based on the quantity of sprayed material when three nozzles are open constantly, where each nozzle spray diameter was 0.33 m and the robot speed was 0.33 m/s (the corresponding speed to expose the target for 1 s of spraying).

4.5 | Experimental design

Twenty male and female students aged 25–40 participated in the experiments and were divided into two groups, one for each marking method (*CDC* and *Free-hand*). Each participant practiced the three collaboration levels. For each collaboration level, the robot traveled a single time along the target base with steps of 1 m. The image switching time was set to 12 s.

For the fourth collaboration level (autonomous) the robot performed 10 repetitions, in each of which the robot traveled along the target's base with 1 m intervals, captured the target's frame, analyzed the captured frame using the artificial target detection algorithm, and sprayed toward each of the detected targets.



FIGURE 11 Target detection and FP results. Original captured image (left), detected target (middle), and detected target with added FP (right)

5 | RESULTS AND DISCUSSION

The experimental results are summarized in Figure 15, Figure 16, and Table 1, where the graph bars “marking comparison—TP” and “marking comparison—FP” represent the TP and FP rates, respectively, using the *Marking comparison* spray evaluation; the bars “spraying comparison—TP” and “spraying comparison—FP” represent the TP and FP rates, respectively, using the *Spraying comparison* spray evaluation; and the “qualitative evaluation” bar represents the TP rate using the *Qualitative evaluation* spray evaluation, as described in Section 4.4. For ease of comparison, Figures 15 and 16 also present results of collaboration level 4, which are identical in both figures.

The overall performance of the *Free-hand* marking method was better than the *CDC* marking method [$t(7)$, $p < 0.005$] by 2.8% on average. TP rate was improved for all cases [$t(7)$, $p < 0.005$] when using the *Free-hand* marking method (except for the *qualitative evaluation* in collaboration level 2). However, along with the improvement of the TP rate, the FP rate increased by 4.5% on average, implying more wasted spraying material. In both marking methods, the TP and the FP rates increase

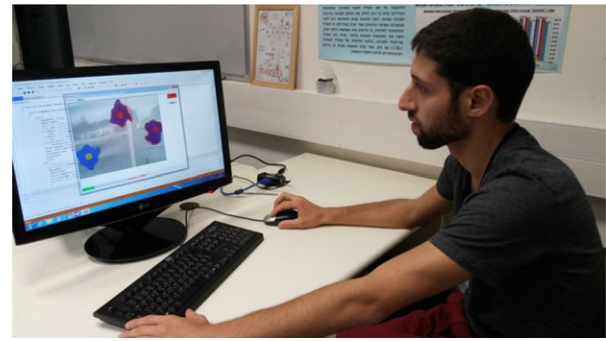


FIGURE 12 Human marking targets using a remote computer in Beer-Sheva, Israel, 90 km south of the robot

when transforming from collaboration level 2 to level 3 [$t(7)$, $p < 0.05$]. The best TP rate results (91.3% on *Marking comparison* and 93.6% on *Spraying comparison*) were achieved when using the *Free-hand* marking method with collaboration level 3. Best minimization of FPs was achieved for the *CDC* marking method, while using collaboration level 1 (3.8% on *Marking comparison* and 10.1% on *Spraying comparison* with

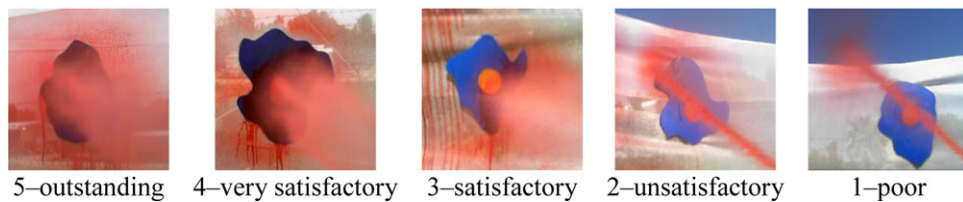


FIGURE 13 Target spraying evaluation scale 5 (outstanding) → 1 (poor)

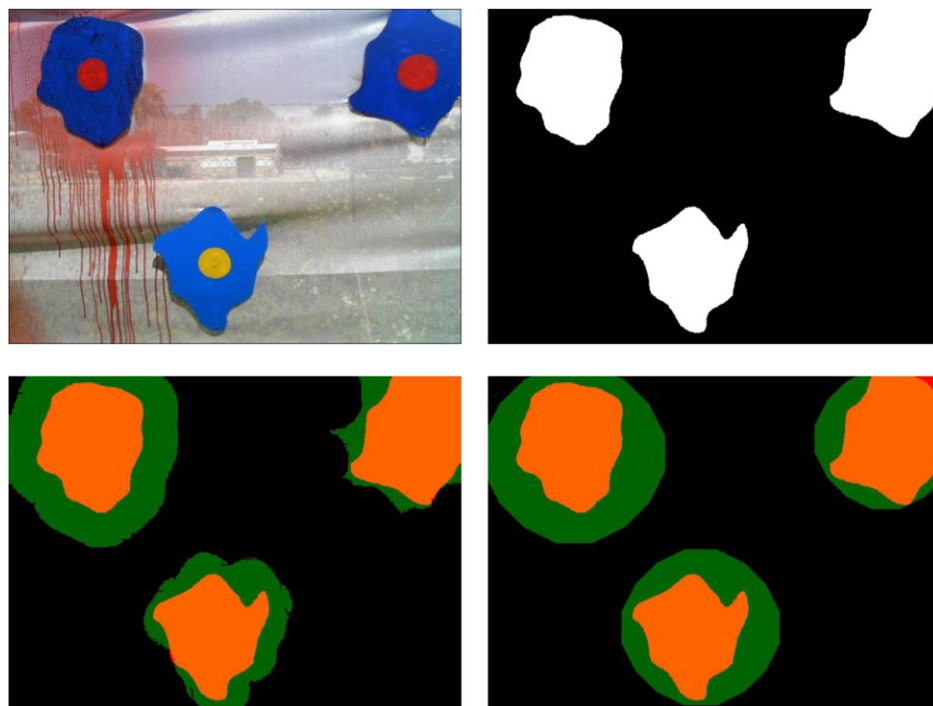


FIGURE 14 Spray evaluation while using the *CDC* marking method with the third collaboration level. Captured image from the spraying site (upper left), computer detected (for the spray evaluation both the red and yellow midtarget circles were calculated) (upper right), comparison between the human and robot marked areas colored green, and the computer-detected targets in the image colored red (lower left), and comparison between the theoretical sprayed areas while using the *ASE* colored green and the computer-detected targets in the image colored red (lower right)

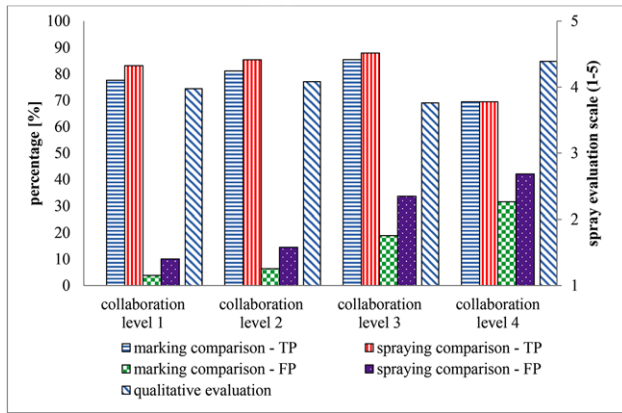


FIGURE 15 Experimental results for the *CDC* marking method

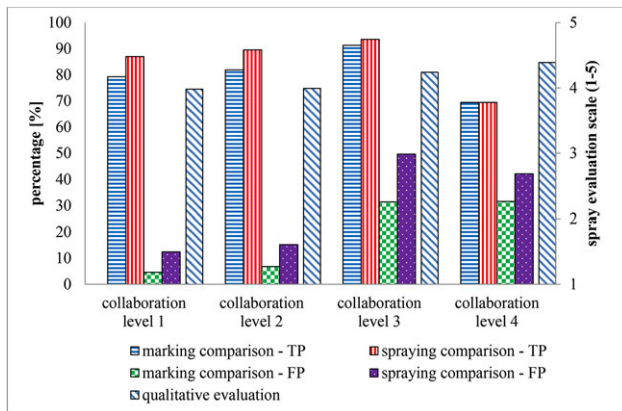


FIGURE 16 Experimental results for the *free-hand* marking method

standard deviations of 1.8 and 3.3, respectively). However, in this case the TP rate was 77.6%.

Another important parameter to be considered for actual implementation is the number of sprays (Table 2). The number of sprays also represents the number of detected targets sprayed where each target

is sprayed once. Since the number of targets in each repetition was 50, we can see that some false spraying occurs in all the repetitions. One of the reasons that the number of sprays is higher while using the *Free-hand* marking method is due to the marking procedure. For future commercial use, we recommend filtering out small objects in the marked image, which should not be considered as targets to be sprayed due to their small size.

During the experiment, the robot traveled a total distance of 1,044 m (16 users \times 3 repetitions per user \times 18 m for each repetition + 10 repetitions \times 18 m for each repetition), captured 1,108 frames, and sprayed 3,378 targets. The experiment shows that collaboration of a human in the spraying process is feasible and improves the spraying process. Collaboration between the remote robot and the human resulted in improved TP and FP rates (TP rate increased by 13.4% and FP rate decreased by 19.5% with statistical significance at $p < 0.05$), compared to a fully autonomous operation (collaboration level 4).

The spraying material estimation analyses (Table 3) revealed that in each of the collaboration levels and marking methods, the decrease in spraying liquid is more than 50%. Table 3 shows that while the robot operated in autonomous mode, the average liquid used was less than in the *CDC* and *free-hand* marking methods (for all collaboration levels), although the FPs of the autonomous level were the highest (Table 1). This low liquid level can be explained by the number of detectable and undetectable targets (Fig. 10) combined with the fact that while operating autonomously, the robot does not detect and spray the undetectable targets. Additional evidence of this is the number of sprays the robot applied in each collaboration level (Table 2).

6 | CONCLUSIONS

This research presented a collaborative human-robot framework for site-specific spraying of grape cluster targets. An experiment to evaluate the elements of the collaborative human-robot framework

TABLE 1 Summary of results

Marking method	Collaboration method	Average marking comparison - TP (%) (std)	Average marking comparison - FA (%) (std)	Average spraying comparison - TP (%) (std)	Average spraying comparison - FA (%) (std)	Average qualitative evaluation - TP (std)
CDC	1	77.6 (10.1)	3.8 (1.8)	83.1 (9.8)	10.1 (3.3)	4 (0.3)
	2	81.1 (5)	6.4 (2.6)	85.3 (5.1)	14.5 (3.5)	4.1 (0.3)
	3	85.4 (5)	18.9 (8.4)	87.9 (4)	33.7 (11)	3.8 (0.4)
Free hand	1	79.3 (8.5)	4.6 (3.6)	87 (5.4)	12.4 (7.9)	4 (0.3)
	2	81.9 (9.9)	6.8 (5.4)	89.5 (5.6)	15.2 (9.6)	4 (0.3)
	3	91.3 (6.6)	31.4 (4.9)	93.6 (5.1)	49.6 (11.2)	4.2 (0.3)
None	4	69.4 (19.7)	31.5 (14.6)	69.5 (19.7)	42.1 (38.6)	4.4 (0.7)

TABLE 2 Number of sprays

Marking method	Number of sprays (std)			
	Collaboration 1	Collaboration 2	Collaboration 3	Collaboration 4
CDC	57.5 (6.2)	55.0 (5.9)	67.0 (7.2)	41.3 (1.9)
Free hand	64.4 (6.9)	66.4 (7.1)	60.4 (6.5)	

TABLE 3 Spraying material usage estimation

Collaboration level	CDC			Free hand			Autonomous	Continuous driving
	1	2	3	1	2	3	4	
Liquid use (l)	3.06	2.93	3.57	3.43	3.54	3.22	2.20	8.72
Liquid reduction compared to continuous driving (%)	64.86	66.39	59.06	60.66	59.44	63.10	74.76	

working in sync was designed, implemented, and evaluated. The experiment proves the feasibility of human-robot collaboration for the complex task of targeted spraying considering both TP and FP rates. The collaborative spraying system reduces the quantity of sprayed material by 50%, which has both economic and environmental impacts.

Results obtained can be used to implement a human-robot operational system by deciding on the best target marking method and collaboration level according to the selected criterion. For example, if TP rate is prioritized, full manual collaboration should be employed with a CDC marking method. To achieve the lowest FP rate, collaboration level 2 should be employed using the *free-hand* marking method. This is important since in the spraying task the selected criterion can change throughout the season depending on pests and environmental and growing conditions. For example, when there is a high risk of dangerous pests, it is more important to ensure high coverage of targets (maximize TP rate) than wasted material (FPs). When risks are low, the farmer prefers to limit spray material as much as possible (minimize FPs).

It must be noted that spraying evaluation in this paper focused on the human collaboration aspects for target detection (specifically on the marking method and collaboration levels). Future work should focus on evaluating spraying performance for different spraying characteristics (e.g., droplet size, droplet spread, and spraying materials) for specific crops, pests, and pesticides. Additionally, human-robot collaboration for other tasks can be developed and incorporated into the site-specific sprayer (e.g., navigation along the row, trimming). In this research, timing issues such as robot driving speed, marking time, and time for the ASD to spray each target were not optimized; these can be improved and will yield increased robot productivity. Additional future work can concentrate on improving the human remote perception by adding advanced sensors (e.g., stereo vision, 3D cameras, and a combination of RGB and LIDAR) and evaluating the robotic sprayer performance in real-world conditions. It must be noted that if sensors are added, efficient design methods must be employed to display the sensed information so as to maximize information display while minimizing distraction. Hence this is an area recommended for future research.

The remote interface for the human operator was designed with great simplicity under the assumption that a supervisor is present during the experiments. An advanced remote human interface can be developed in future work. We suggest that such an interface be implemented on a web platform to allow human control from different devices, such as smart phones, hand-held computers, tablets, and laptops. Another subject for future work related to the interface design can be the evaluation of different pointing devices such as a touch

screen, a 3D mouse, and a digital pen, and their effect on the human marking performance. This is similar to what was investigated recently by Adamides²⁵ for teleoperation tasks.

Future work can also focus on the image switching time and try to determine the optimal time for best target marking. This can include a comparison of constant switching times compared to switching times that are set by the user when he/she completes the marking task.

With minor adaptations, the human-robot collaborative framework can be easily used with other agricultural applications, such as fruit picking, yield and disease monitoring, and field exploration. For full robot operation, crop-specific target detection (e.g., Ref. 38) and navigation algorithms (e.g., Ref. 39) must be integrated. The framework can also be used in other commercial applications that require complex target detection, such as border control and hazardous material environment.

ACKNOWLEDGMENTS

This research was supported by Helmsley Charitable Trust through the Agricultural, Biological and Cognitive Robotics Initiative, and by the Rabbi W. Gunther Plaut Chair in Manufacturing Engineering, both at Ben-Gurion University of the Negev.

REFERENCES

- Singh S, Burks TF, Lee WS. Autonomous robotic vehicle development for greenhouse spraying. *Trans ASAE*. 2005;48(6):2355–2361.
- Cho SI, Ki NH. Autonomous speed sprayer guidance using machine vision and fuzzy logic. *Trans ASAE*. 1999;42(4):1137–1144.
- Swan SH, Kruse RL, Liu F, et al. Semen quality in relation to biomarkers of pesticide exposure. *Environ Health Perspectives*. 2003;111(12):1478–1484.
- Slaughter D, Giles D, Downey D. Autonomous robotic weed control systems: A review. *Comput Electron Agricult*. 2008;61(1):63–78.
- Lee WS, Slaughter D, Giles D. Robotic weed control system for tomatoes. *Precision Agricult*. 1999;1(1):95–113.
- Elkabetz P, Edan Y, Grinstein A, et al. Simulation model for evaluation of site-specific sprayer design. Paper presented at the ASAE Annual International Meeting, Orlando, FL; 1998.
- Gil E, Escol A, Rosell JR, et al. Variable rate application of plant protection products in vineyard using ultrasonic sensors. *Crop Protection*. 2007;26(8):1287–1297.
- Goudy HJ, Bennett KA, Brown RB, et al. Evaluation of site-specific weed management using a direct-injection sprayer. *Weed Science*. 2001;49(3):359–366.
- Edan Y, Kondo N, Shufeng H. Automation in agriculture. In: Nof SY, ed. *Handbook of Automation*. Berlin: Springer-Verlag; 2009:1092–1128.

10. Nishiwaki K, Amaha K, Otani R. Development of nozzle positioning system for precision sprayer. Paper presented at the Automation Technology for Off-Road Equipment, Kyoto, Japan; 2004.
11. Oberti R, Marchi M, Tirelli P, et al. Selective spraying of grapevines for disease control using a modular agricultural robot. *Biosyst Eng*. 2016;146:203–215.
12. Bac CW, Henten EJ, Hemming J, et al. Harvesting robots for high-value crops: State-of-the-art review and challenges ahead. *J Field Robotics*. 2014;31(6):888–911.
13. Jeon HY, Tian LF, Grift T. Development of an individual weed treatment system using a robotic arm. Paper presented at the ASABE Annual International Meeting, Tampa, FL; 2005.
14. Shapiro A, Korkidi E, Demri A, et al. Toward elevated agrobotics: Development of a scaled-down prototype for visually guided date palm tree sprayer. *J Field Robotics*. 2009;26(6):572–590.
15. Song Y, Sun H, Li M, et al. Technology application of smart spray in agriculture: A review. *Intell Autom Soft Comput*. 2015;21(3):319–333.
16. Kapach K, Barnea E, Mairon R, et al. Computer vision for fruit harvesting robots—State of the art and challenges ahead. *Int J Computat Vision Robotics*. 2012;3(1):4–34.
17. Gongal A, Amatya S, Karkee M, et al. Sensors and systems for fruit detection and localization: A review. *Comput Electron Agricult*. 2015;116:8–19.
18. Jimenez A, Ceres R, Pons J. A survey of computer vision methods for locating fruit on trees. *Trans ASAE*. 2000;43(6):1911–1920.
19. Correa C, Valero C, Barreiro P, et al. Feature extraction on vineyard by Gustafson Kessel Fcm and K-means. Paper presented at the 16th IEEE Mediterranean Electrotechnical Conference (MELECON), Yasmine Hammamet, Tunisia; 2012.
20. Blackmore S, Have H, Fountas S. A specification of behavioural requirements for an autonomous tractor. Paper presented at the 6th International Symposium on Fruit, Potsdam, Germany; 2001.
21. Fong T, Thorpe C. Vehicle teleoperation interfaces. *Auton Robots*. 2001;11(1):9–18.
22. Rodriguez G, Weisbin CR. A new method to evaluate human-robot system performance. *Auton Robots*. 2003;14(2):165–178.
23. Bechar A, Edan Y. Human-robot collaboration for improved target recognition of agricultural robots. *Indust Robot*. 2003;30(5):432–436.
24. Murakami N, Ito A, Will JD, et al. Development of a teleoperation system for agricultural vehicles. *Comput Electron Agricult*. 2008;63(1):81–88.
25. Adamides G. *User interfaces for human-robot interaction: Application on a semi-autonomous agricultural robot sprayer*. Ph.D. thesis, Open University of Cyprus, Information and Communications Systems, Nicosia, Cyprus; 2016.
26. Adamides G, Christou G, Katsanos C, et al. Usability guidelines for the design of robot teleoperation: A taxonomy. *IEEE Trans Human-Machine Syst*. 2015;45(2):256–262.
27. Adamides G, Katsanos C, Christou G, et al. Human-robot interaction in agriculture: Usability evaluation of three input devices for spraying grape clusters. Paper presented at the Sustainable Agriculture through ICT Innovation (EFITA-WCCA-CIGR), Turin, Italy; 2013.
28. Berenstein R. *A human-robot cooperative vineyard selective sprayer*. Unpublished Ph.D. thesis, Ben-Gurion University of the Negev, Industrial Engineering and Management, Beer-Sheva, Israel; 2016.
29. Sheridan TB. *Telerobotics, Automation, and Human Supervisory Control*. Cambridge, MA: The MIT Press; 1992.
30. Berenstein R, Edan Y. Evaluation of marking techniques for a human-robot selective vineyard sprayer. Paper presented at the International Conference of Agricultural Engineering (CIGR-AgEng), Valencia, Spain; 2012a.
31. Berenstein R, Edan Y, Ben Halevi I. A remote interface for a human-robot cooperative vineyard sprayer. Paper presented at the International Society of Precision Agriculture (ICPA), Indianapolis, IN; 2012.
32. Berenstein R, Edan Y. Human-robot cooperative precision spraying: Collaboration levels and optimization function. Paper presented at the Symposium on Robot Control (SYROCO), Dubrovnik, Croatia; 2012b.
33. Berenstein R, Edan Y. Automatic adjustable spraying device for site-specific agricultural application. *IEEE Trans Autom Sci Eng*. 2017;PP(99):1–10.
34. Vitzrabin E, Edan Y. Changing task objectives for improved sweet pepper detection for robotic harvesting. *IEEE Robotics Autom Lett*. 2016;1(1):578–584.
35. Oren Y, Bechar A, Edan Y. Performance analysis of a human-robot Collaborative target recognition system. *Robotica*. 2012;30:813–826.
36. Zaidner G, Shapiro AA. Novel data fusion algorithm for low-cost localisation and navigation of autonomous vineyard sprayer robots. *Biosyst Eng*. 2016;146:133–148.
37. Berenstein R, Edan Y. Robotic precision spraying methods. Paper presented at the ASABE Annual International Meeting, Dallas, TX; 2012c.
38. Berenstein R, Shahar OB, Shapiro A, et al. Grape clusters, foliage detection algorithms for autonomous selective vineyard sprayer. *Intell Serv Robotics*. 2010;3(4):233–243.
39. Rovira-Más F, Millot C, Sáiz-Rubio V. Navigation strategies for a vineyard robot. ASABE Annual International Meeting. Orleans, LA; 2015.

SUPPORTING INFORMATION

Additional Supporting Information may be found online in the supporting information tab for this article.

How to cite this article: Berenstein R, Edan Y. Human-robot collaborative site-specific sprayer. *J Field Robotics*. 2017;34:1519–1530. <https://doi.org/10.1002/rob.21730>